Precision Measurement of the Magnetic Moment of the Proton in Units of the Nuclear Magneton with High Velocity Particles

by **H. Gubler, S. Münch** and **H. H. Staub**

Physik Institut der Universität Zürich

(16. VIII. 73)

Zusammenfassung. Die vollständigen und abschliessenden Versuche zur Präzisionsbestimmung des magnetischen Momentes des Protons in Einheiten des Kernmagnetons mit hochenergetischen H^+ und He^+ Ionen mit dem absoluten Laufzeitspektrometer und dem absoluten 180° magnetischen Spektrographen werden beschrieben. Die detaillierte Untersuchung möglicher systematischer Fehler ergab keine signifikante Aenderung des früher erhaltenen Wertes, aber einen reduzierten Wert des totalen möglichen Fehlers. Der vorliegende Wert von μ'_P/μ_n gemessen an einer sphärischen Probe mit reinem H_2O, unkorrigiert für diamagnetische Abschirmung, ist

$$\mu'_P/\mu_n = 2{,}792777 \pm (20); \quad 7 \text{ p.p.m.}$$

in vorzüglicher Uebereinstimmung mit dem früheren, vorläufigen Wert und neueren und zum Teil genaueren Werten, die mit anderen Methoden erhalten wurden.

I. Introduction

Marion and Winkler [1] pointed out that there existed a small but systematic difference between the values of a number of nuclear resonance and threshold energies measured by magnetic deflection and velocity determination by time of flight methods. Attributing the difference to an error in the currently accepted value μ'_P/μ_n of the proton magnetic moment in units of the nuclear magneton they gave a value for this quantity which was quite low but due to its large uncertainty was compatible with three of the more accurate low values [2–4] but was outside the two high values of Mamyrin and Frantsuzov [5] and Boyne and Franken [6]. They suggested that the accuracy of the experiment could be considerably improved, perhaps to 20 p.p.m., by operating the time of flight velocity gauge and the magnetic spectrometer simultaneously and without taking recourse to a nuclear reaction.

Just at this time the new and highly accurate determinations of e/h from the Josephson effect [7] seemed to indicate a systematic difference between the values of the fundamental atomic constants determined from experiments involving quantum electrodynamics and those without. Moreover there was increasing evidence that the determination of the Faraday number F, which represents one of the important input data for the adjustment of the fundamental constants, is subject to serious difficulties with electrochemical measurements whereas μ_P/μ_n, together with γ_P, the gyromagnetic ratio of the proton, furnishes a rather accurate value of F.

In 1969 the absolute time of flight velocity gauge built by Seagrave, Brolley and Beery [8], following closely the original design of Altar and Garbuny [9], was brought

to the University of Zürich to perform such a measurement in conjunction with the absolute magnetic spectrometer of our laboratory. After a few but important changes in the construction of the velocity gauge a preliminary result, subject to possible systematic errors of less then 15 p.p.m., $\mu'_P/\mu_n = 2.792771 \pm 0.000031$, was presented at the Gaithersburg Conference [10].

In this paper we present an account of the investigation of the possible sources of systematic errors and the final result with increased accuracy.

II. Instrumentation

Figure 1a shows schematically the experimental layout and Figure 1b its block diagram. A beam of highly monoenergetic protons (1.285 MeV) or He$^+$ ions (0.985 MeV) from an electrostatic generator is passed through a plane parallel plate electric
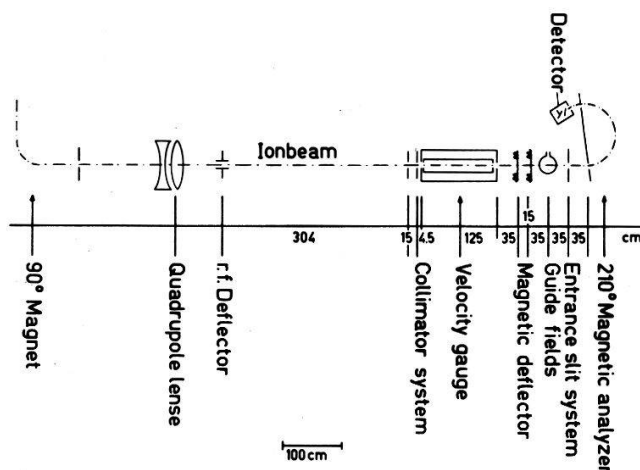
Figure 1a
Instrumental arrangement. Distances in cm.

deflector 4 cm long and with a plate distance of 0.4 cm to which a harmonic r.f. voltage up to 100 V amplitude at a frequency $\omega_0/4\pi = 34.5$ MHz is applied. At a distance of 304 cm from the centre of the deflector a circular collimator opening of 1.2 mm diameter is placed on which the undeflected beam is focused by a quadrupole lens preceding the deflector. The collimator opening is followed by a antiscattering diaphragm of slightly larger diameter (1.3 mm). This collimator system is electrically insulated from the velocity gauge and kept at a positive potential of at least +40 V relative to the latter.

The velocity gauge proper was that built and described by Seagrave et al. [8] and West [11]. However, several minor but quite important alterations had to be made in order to make a measurement of some parts per million accuracy possible.

Referring to Figure 1 of Ref. [8], the inner field gap electrodes, the quartz spacer and the outer field gap electrodes were pressed by the outer cavity end-plates on the drift tube by means of tension springs attached to the outer cavity cylinder wall. The end-plates could move with friction fit within the outer cavity cylinder. This construction suffers from a number of serious difficulties. (i) Any temperature variation or
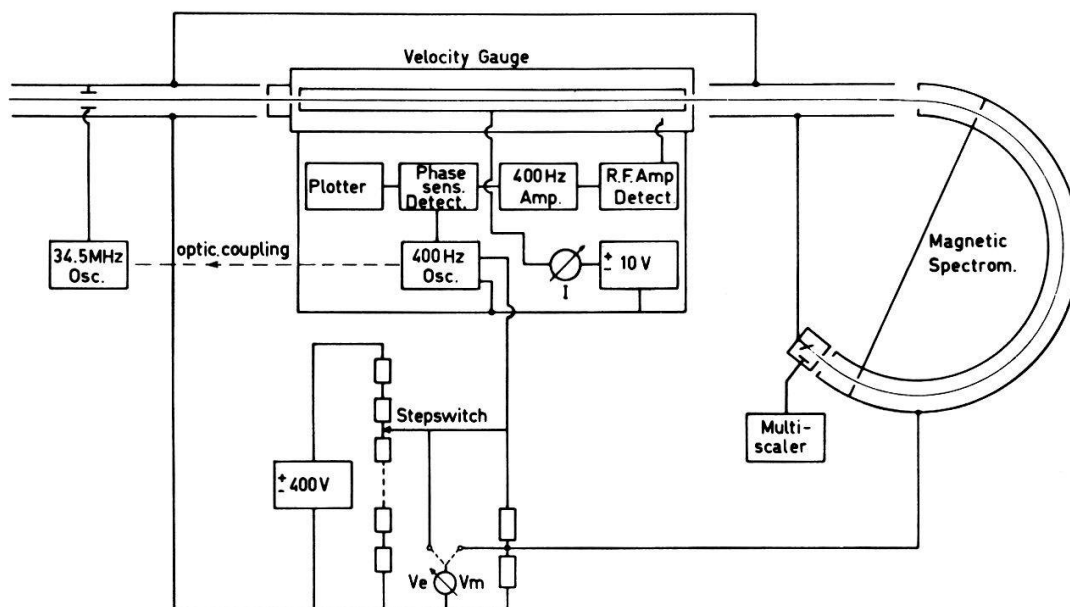
Figure 1b
Block diagram of velocity gauge and magnetic spectrometer.

mechanical vibration can lead to tilting and jamming of the end-plates, whereby the effective electric length of the gauge is seriously changed, even if the normal mode frequencies might only be little affected. But since it is the forced electromagnetic oscillation of the cavity which one observes, small changes of the normal mode frequencies have little effect while the occurrence of the interference minimum excited by the passage of an intensity modulated charged particle beam is determined by the electrical length. (ii) The geometrical length of the cavity must be inferred from the rather ill-defined length of the drift tube after disassembling the cavity.

The new design is shown in Figure 2. A section of the outer cavity end-plates is firmly attached to the drift tube, by means of teflon screws, through holes in the quartz spacers. The outer field gap electrode is pressed against the optically flat outer face of the quartz spacer with spring washers by a retainer. Contact of the end-plate section to the remainder of the outer cavity structure is made by a ring of high-frequency contact springs. With this arrangement it was possible to measure the distance of the outer quartz surfaces as it exists during the experiment without disassembling the cavity except for the removal of the outer gap electrode. This change immediately gave an enormous gain in stability and reproducibility of the resonance minima. On the other

Figure 2
Construction of cavity end and field gaps.

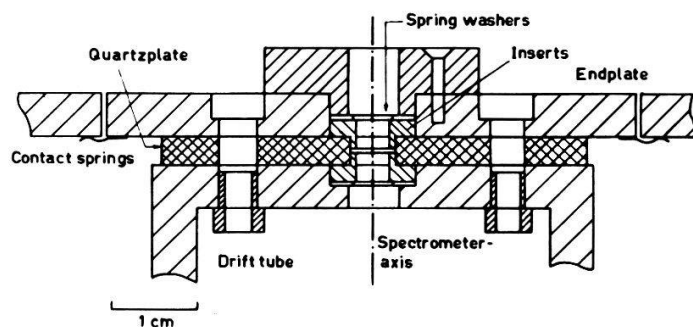hand the change reduced the Q value of the cavity from about 4000 to 1800. This was presumably caused by the spring contacts and had no serious consequences (cf. Section IV). The diameter of the gap opening was increased from 3 to 4 mm, the gap distance decreased to 0.4 mm.

The entire velocity gauge with its vacuum jacket and the signal detector assembly was mounted on an insulated table to which d.c. and a.f. (400 c.p.s.) voltages up to 1 kV could be aplied. This was necessary since the application of voltages to the drift tube alone would lead to radical changes of the secondary electron currents (cf. Section IV), resulting in large shifts of the interference minima.

After leaving the velocity gauge the beam was guided through a region of ground potential by a system of Helmholtz coils and was magnetically swept at 50 Hz across a rectangular entrance diaphragm 1.2 by 6 mm followed by a 2 mm circular opening of the magnetic analyser. In this manner we obtained the necessary intensity reduction of the beam but also averaged out any velocity differences of the particles within the beam caused by the dispersion of the 90° magnet following the accelerator and by the r.f. modulation deflector. The ions then entered the vacuum chamber of the magnetic 210° spectrometer. This instrument has been described in detail by Winkler and Zych [12]. The only changes made were (i) the electrical insulation of the vacuum chamber, including the slit system, in order to determine the ion velocity at fixed magnetic field; (ii) a new slit system of high precision was used. It consisted of a solid circular bar of sintered molybdenum (1.4 cm diameter) into which the inner jaws of the defining slits were machined, ensuring thereby an unalterable distance of about 100 cm and straightness of the inner slit edges. The outer jaws were adjustably fixed on the molybdenum rod. Outside the vacuum chamber the molybdenum rod carried a jacket for cooling with air or water and temperature sensors (N.T.C. resistors) at both entrances into the vacuum chamber and at the centre of the rod. After leaving the magnet vacuum chamber the ions entered a small scattering chamber at ground potential where they were scattered by a nickel foil under a fixed angle on a silicon surface barrier detector.

The magnetic field was kept constant by a stabilizing n.m.r. probe consisting of a spherical sample of 1.2 cm diameter containing a 1/40 molar solution $MnSO_4$ located at a radial distance of 52.5 cm (2.5 cm outside the nominal particle orbit) and at an angular distance of 106° from the entrance slit. By this probe the field was stabilized via its current generator to better then 1 p.p.m. This corresponds to about 1/30 of the full width of the n.m.r. signal.

The stationary r.f. signal maintained by the passage of the ions through the two field gaps of the velocity gauge was picked up by a radial stub antenna of 4.5 cm length. Originally the signal was a.f. amplitude modulated by a 400 Hz amplitude modulation of the deflecting r.f. voltage. For the final measurements the a.f. amplitude modulation was replaced by phase modulation obtained by adding a 400 Hz harmonic voltage with about 35 V amplitude to the d.c. voltage applied to the velocity gauge. The use of velocity or phase modulation results in two considerable advantages: (i) The large amplitude modulation, index $m \approx 0.5$, will inevitably lead to weak phase or frequency modulation which can cause slight shifts of the interference minimum. Velocity modulation results in a phase modulation index of order 10^{-5}. Consequently the higher side bands are entirely negligible and the interference minimum is differentially swept. (ii) This leads to a true null voltage at the interference minimum whose vicinity can be observed with maximum sensitivity of the detector without danger of saturation. A.f. amplitude modulation however was used for locating the minima approximately and also for the elimination of background signals (Section IV). R.f. coupling between the

a.f. oscillator located on the velocity gauge was minimized by effecting the coupling via a light beam.

The signal picked up by the stub antenna was fed to a radio receiver (Rhode and Schwarz E.S.M.) with 60 Ω input impedance and a 0.5 μV noise level. Its r.f. amplifier had a band width of 40 kHz. Its square law detector was followed by a conventional a.f. amplifier and a stage tuned to 400 Hz with a bandwidth of 3 Hz whose output was fed to a conventional phase sensitive detector with a time constant of 3 sec.

III. Experimental Procedure

The quantity μ'_P/μ_n is determined by the Larmor precession frequency ω_m of the protons in the magnetic field B measured by the momentum of the ions whose velocity is determined with the velocity gauge. Measurements were taken at fixed energy of the ions, protons or He$^+$, from the accelerator at fixed frequency of the deflecting r.f. voltage equal to one-half the fundamental T.M. mode frequency of the velocity gauge and at fixed magnetic field B of the magnetic spectrometer by applying voltages V_e and V_m to the velocity gauge and the magnetic spectrometer vacuum chambers respectively. These voltages were simultaneously applied in steps of about 30 V to the velocity gauge and of 20 V to the magnetic spectrometer over a region from -400 to $+400$ V. If $v_0 = \beta_0 c$ is the mean velocity of the ion in the velocity gauge, M its rest mass, m the proton rest mass, D the mean slit distance of the magnetic spectrometer, μ'_P/μ_n is given by:

$$\mu'_P/\mu_n = \frac{D\omega_m}{2c} \frac{m}{M} \left[\left(\frac{1}{\sqrt{1-\beta_0^2}} + \frac{V_e - V_m}{Mc^2} \right)^2 - 1 \right]^{-1/2}$$

$$\approx \frac{D\omega_m}{2c} \frac{m}{M} \frac{\sqrt{1-\beta_0^2}}{\beta_0} \left(1 - \frac{V_e - V_m}{Mc^2 \beta_0^2} \sqrt{1-\beta_0^2} \right). \tag{1}$$

In the last expression quadratic and higher power relativistic terms in $V_e - V_m$ have been neglected since they contribute less than 10^{-6}. The velocity v_0 is given by the phase shift

$$\Phi = \frac{\omega_0 L_0}{v_0}$$

between the current at the entrance and the exit gap effectively spaced by the distance L_0. Ideally this phase shift is $\Phi_0 = (2N - 1)\pi$, an odd integer multiple of π for an interference minimum of the cavity oscillation and $2N\pi$ for a maximum. If velocity modulation is used zero output signals (cf. Appendix) are observed at these values.

For the present measurements the fundamental principal mode frequency of the cavity was about 69 MHz, the effective length L_0 125 cm, and D about 100 cm. These data result in the following convenient values (Table I) for the energy E_0 of the H$^+$ and He$^+$ ions with a large ratio of N. The current through the gauge was about 1 μA with a r.f. modulation of 20 to 50%.

The determination of the null signal of the cavity was carried out by applying V_e, in steps of about 30 V from -400 to $+400$ V, to the velocity gauge to which, in addition, the 400 Hz velocity modulation with an amplitude of 35 V was applied. Each voltage step was left for 3 sec and the output voltage of the phase sensitive detector recorded by

a plotter. Preceding each voltage step the plotter was switched off for 0.5 sec to provide step markers. The collimator slit system was kept at a constant positive potential of 85 V to retain the large number of secondary electrons originating at the collimator. In order to eliminate the effect of secondary electrons from the gap electrodes (cf. Section IV) passages through the null signal were made with positive and negative voltages of 9 V on the drift tube relative to the outer conductor of the cavity and only those measurements were accepted which showed the proper shift of + or −9 V in the null passage.

Table I

	E_0 (MeV)	v_0 (cm/s)	$2N - 1$	$\omega_0/2\pi$ (MHz)	B (Gauss)
H^+	1.282	$1.566 \cdot 10^9$	11	13.93	3272
He^+	0.986	$0.690 \cdot 10^9$	25	24.37	5728

Simultaneously the reduced voltage steps were applied to the magnetic spectrometer and the number of ions recorded in the corresponding channel of a multi-channel analyser assigned to each voltage step in order to determine the velocity profile of the incident ions.

A typical example of the voltage step sequence, the output amplitude of the velocity gauge and the velocity profile recorded by the magnetic spectrometer is shown in Figure 3.

Before and after each series of measurements, consisting of four passages across the interference minimum, the absence of spurious background signals was ascertained.
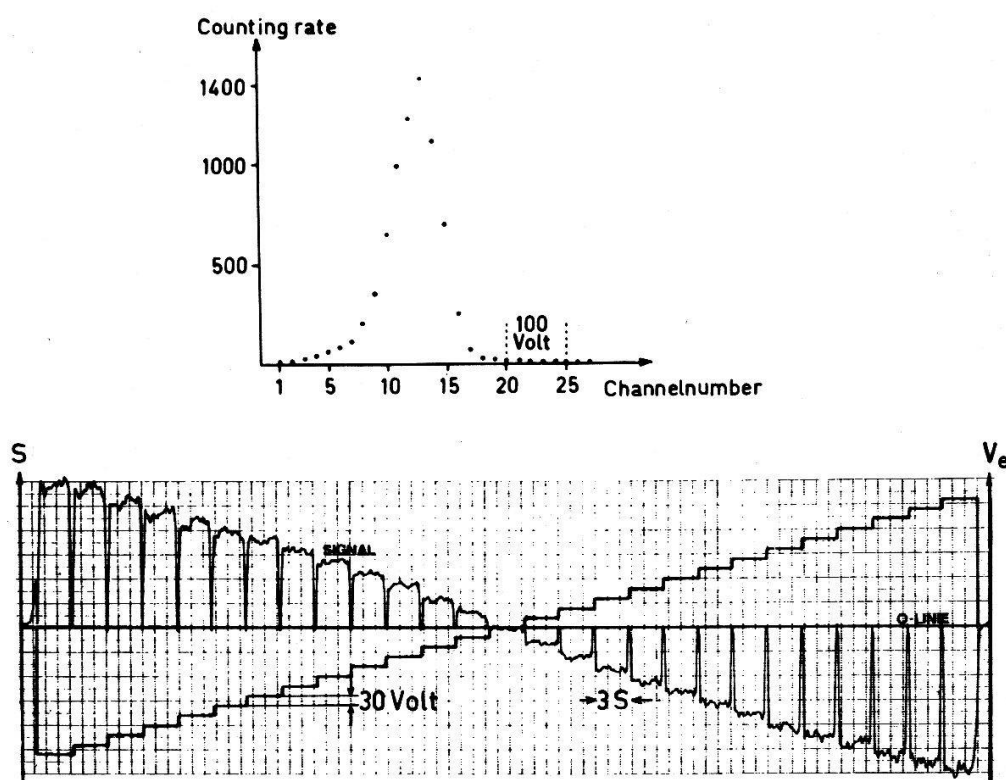

Figure 3
Typical record of step voltages, v modulated gauge signal output and velocity profile.

For this purpose the ion beam was stopped before the collimator. The r.f. deflecting voltage was about 30% amplitude modulated with 400 Hz by optically coupling the a.f. oscillator with the r.f. deflecting voltage oscillator. The output of the phase sensitive detector was then recorded with the amplifier gain increased by about a factor of 5. If no shift relative to the zero signal line was observed the effect of background signal was negligible. A typical example is shown in Figure 4.

Before and after each set of measurements, usually consisting of three series of null passages, the magnetic spectrometer vacuum chamber was removed and the magnetic field configuration was determined with a n.m.r. probe identical to the one used for field stabilization carried along the nominal orbit of the ions over an angle θ of 200° in steps of 4°. Its frequency difference $\Delta(\theta)$ against that of the stabilizing probe ω_m^0 gives the Hartree correction sufficient to first order

$$\omega_m - \omega_m^0 = \tfrac{1}{2} \int_0^\pi \Delta(\theta) \sin \theta \, d\theta.$$

Whereas the determination of the two frequencies ω_0 and ω_m to better then 1 p.p.m. offers no difficulties, particularly since only their ratio and not their absolute values
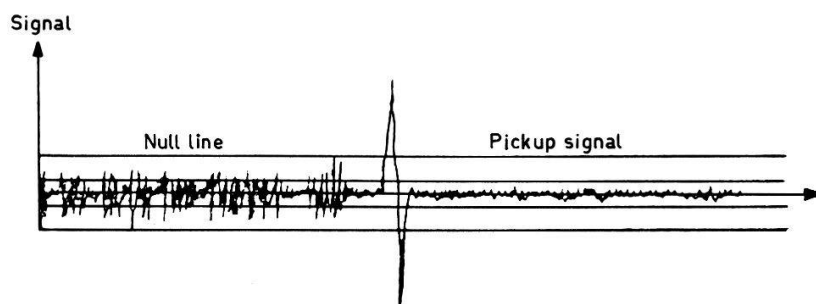

Figure 4
Typical record for determination of zero line. To the right of the marker the ion beam was stopped before the gauge.

enter in equation (1), the measurement of the two lengths D and L_0 requires some attention although it is again only their ratio which is relevant. Indeed the errors of these lengths contribute substantially to the final uncertainty. In principle this could be avoided by using the velocity gauge cavity as the vacuum chamber of the magnetic spectrometer. This however would lead to considerable technical difficulties.

The final measurements of the lengths D and L_0 were carried out on a longitudinal laser interference comparator (H.P. 525 B) at the 'Eidgenössische Amt für Mass und Gewicht'. The effective length L_0 of the cavity (cf. equation (5), Appendix) is the distance between the electrostatic centres of the entrance and exit gaps which coincide with the gap midpoints, provided the gaps are electrically symmetrical with respect to the plane perpendicular to the axis through the midpoint. The gap width was 0.4 mm and the diameter of the circular opening was 4.0 mm. The inserts forming the gap were geometrically symmetrical up to a distance of 6 mm from the midplane. A point by point calculation of the electrostatic field configuration showed that the remaining asymmetries shift the electrical centre by less than 1 μm from the midpoint. After removing the outer inserts, steel gauge blocks with a diameter of 8 mm and optically flat ends carrying reference lines on their surface were attached without any adhesive to the outer faces of the quartz plates. The distance between the reference lines gives the

distance of the outer quartz end-faces. Appropriate corrections for bending effects on the reference lines off the neutral axis had to be applied. Non-parallelity of the two quartz surfaces caused by inaccuracies in the machining of the drift tube would result in an error of less than 1 μm. The quartz plates and inner gap inserts were then disassembled and the distance of the gap centre relative to the outer quartz surface was measured with a S.I.P. Trioptic feeler gauge. During all measurements temperatures of the critical parts were measured to 0.1° C.

The distance between the inner jaws of the slit system of the magnetic spectrometer was also determined with the laser interference comparator. Effects due to bending of the molybdenum rod are considerably larger than for the drift tube. However, since the slits, which are 0.55 cm off the axis of the rod, are used in a vertical position their midpoints are located in the neutral line and the bending effect results in a non-parallelity of the slits. This simply broadens the velocity profile symmetrically by an irrelevant and negligible amount. The widths of the slits were measured on a conventional comparator. Temperature corrections were of course considerably larger for the molybdenum rod ($\alpha = 5.3 \cdot 10^{-6}/°$) than for the invar drift tube ($\alpha = 1.2 \cdot 10^{-6}/°$).

IV. Sources of Systematic Errors

The three most important sources for systematic errors occurring in the operation of the velocity gauge are:

i) The modification of the value of the null-phase by secondary electrons crossing the field gaps, from $(2N - 1)\pi$ to $\Phi_0 = (2N - 1)\pi + \epsilon$. This shift depends on the place of origin of the secondaries, their velocity and direction of motion and their number, which in turn depends on the number of ions impinging on the walls of the gap electrodes. Their energies range from 0 to about 3 keV, with the great majority below 10 eV, as shown by the d.c. characteristic. In principle the secondary electron current could be determined and minimized by applying a small d.c. voltage V_D between the drift tube and the outer wall of the cavity. No electrons would cross the gap if the current I were found independent of the voltage V_D, in which case the current I would simply be due to high energy positive ions being lost within the drift tube. This current was always of the order of 10^{-3} of the total current traversing the velocity gauge and depended, of course, strongly on the correct positioning of the gauge, the r.f. modulation index and the quality of the vacuum. As is to be expected, the most stable and reproducible
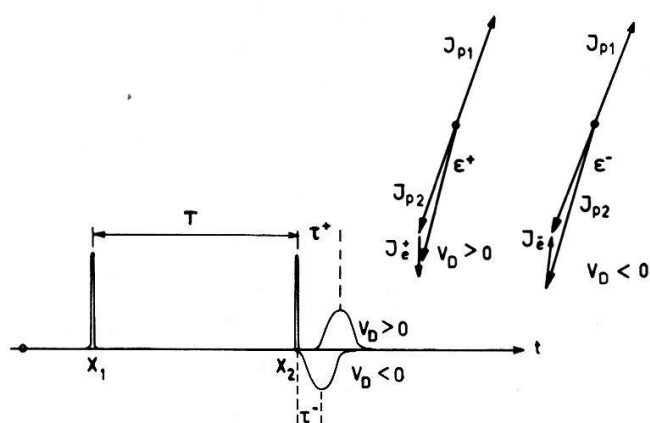

Figure 5
Effect of secondary electrons. Right-hand side: phase relation in complex phase plane.

operation occurs when the ion beam is focused on the first collimator opening and with a positioning of the gauge giving a minimum drift tube current for either polarity of V_D. However, even positioning the gauge so that the current difference, with V_D positive or negative, is unobservable would lead to far too large shifts of the null phase. With the ion beam properly focused on the collimator, appreciable secondary electron currents can only originate at the electrodes of the exit gap. As shown in Figure 5, a pulse of positive ions with velocity v_0 crosses the entrance gap at time 0 and the exit gap at time T. If V_D is positive a corresponding positive low velocity v_e electron pulse originates at time $T^+ + l^+/v_0^+$ and crosses the gap at $T^+ + l^+(1/v_e + 1/v_0^+)$ (see Fig. 5). Conversely, if V_D is negative the electrons originate at a distance l^- in front of the gap centre and cross it in the same direction as the ions thereby producing a negative pulse at $T^- + l^-(1/v_e - 1/v_0^-)$. According to equations (3) and (4) the resulting signal S is:

$$S^+ = |1 + \alpha e^{-i\Phi^+} + \alpha\gamma^+ e^{-i(\Phi^+ + \varphi^+)}|^2; \quad \Phi^+ = \frac{\omega_0 L_0}{v_0^+}; \quad \varphi^+ = \omega_0 \tau^+ = \omega_0 l^+ \left(\frac{1}{v_e} + \frac{1}{v_0^+}\right)$$

$$S^- = |1 + \alpha e^{-i\Phi^-} - \alpha\gamma^- e^{-i(\Phi^- + \varphi^-)}|^2; \quad \Phi^- = \frac{\omega_0 L_0}{v_0^-}; \quad \varphi^- = \omega_0 \tau^- = \omega_0 l^- \left(\frac{1}{v_e} - \frac{1}{v_0^-}\right)$$

with a minimum at:

$$\Phi_0^\pm = (2N - 1)\pi + \epsilon^\pm.$$

Assuming reasonable values:

$$\alpha = 1; \quad \gamma^+ = 5 \cdot 10^{-3}; \quad l^+/L_0 = 2 \cdot 10^{-3}; \quad v_e = 10^8 \text{ cm/s}$$

the systematic error in v_0^+ would amount to over 100 p.p.m.

Since it would be extremely difficult to determine the values of γ, l and v_e, the condition $\epsilon^+ = \epsilon^- = 0$, equivalent to $\gamma^+ = \gamma^- = 0$ since $\varphi^\pm < \pi$, was realized by adjusting the gauge until

$$\Delta = V_e^- - V_e^+ - 2V_D = 0 \pm 6 \text{ V},$$

where $V_e^\pm$ are the step voltages for zero signal output with the drift tube voltage $+$ or $- V_D$ respectively. With this condition an error of $\Delta v/v_0 = 2.3$ p.p.m. for protons is introduced.

ii) Deviation of the null-phase from $(2N - 1)\pi$ due to asymmetries of the eigen-functions. According to equation (3) the voltage developed on the antenna of the velocity gauge at x_0 is given by the Green function

$$G(x_0, x') = \sum_n \frac{\omega_n/\omega_0 \, v_n(x_0) \, u_n(x')}{\omega_0^2 - \omega_n^2 - i\omega_0 \omega_n/Q_n}$$

$$V(x_0) = \text{const} \, (G(x_0, x_1) + KG(x_0, x_2) e^{-i\Phi}),$$

where $K = \gamma(C_1/C_2)$ is a real positive number ≈ 1, and $\Phi = \omega_0 L_0/v_0$ the phase shift over the effective length L_0 with the effective velocity v_0. The output signal of the first

detector is $S \propto |V(x_0)|^2$ and shows a minimum (a.f. amplitude modulation) or a null signal (a.f. v modulation) for

$$\operatorname{tg} \Phi_0 = \frac{G_1^* G_2 - G_2^* G_1}{i(G_1^* G_2 + G_2^* G_1)} = \operatorname{tg}\left((2N-1)\pi + \epsilon\right) \approx \epsilon$$

$$G_1 = G(x_0, x_1); \quad G_2 = G(x_0, x_2).$$

There will therefore always be a shift of the resonance from $(2N-1)\pi$ since G cannot be purely real or imaginary if the cavity is tuned to the lowest mode $\omega_1 = \omega_0$.

Furthermore ϵ will be finite with a finite value of Q since even with perfect geometric symmetry in x_1 and x_2 the eigenfunctions $u_n(x)$ will be alternately symmetric or antisymmetric:

$$u_n(x_1) = \pm u_n(x_2).$$

Assuming exact tuning to ω_1 we separate G in real and imaginary parts:

$$G(x, x') = i(F + f) + g,$$

where F represents the purely imaginary first and large term and f and g the imaginary and real parts of the higher terms. For reasonably high Q:

$$f \ll g \ll F$$

and

$$\epsilon = \frac{g(x_0, x_1) F(x_0, x_2) - g(x_0, x_2) F(x_0, x_1)}{F(x_0, x_1) \cdot F(x_0, x_2)}.$$

Splitting g and F in symmetric and antisymmetric parts with respect to x_1 and x_2

$$g(x_0, x_1) = s_1 + a_1; \quad g(x_0, x_2) = s_1 - a_1$$

$$F(x_0, x_1) = S_1 + A_1; \quad F(x_0, x_2) = S_1 - A_1$$

$$\epsilon = \frac{2(a_1 S_1 - s_1 A_1)}{S_1^2 + A_1^2} \approx \frac{2a_1}{S_1},$$

since $a_1 \ll S_1$ as shown in the complex phase plane in Figure 6. A calculation of this value would necessitate a very accurate knowledge of the eigenfunctions, the tuning conditions and the location of the antenna. The terms in the series for a_1 certainly decrease quite rapidly and it is therefore reasonable to locate the stub antenna at $v_2(x_0) = 0$. An estimate of ϵ, using the capacitance terminated coaxial line model, shows that ϵ can be of the order of several 10^{-4} producing an error of order $\Delta v/v_0 = -\epsilon/(2N-1)\pi \approx 10$ p.p.m. and that even a large increase in Q would not remedy the situation. One has therefore to resort to measurements with two different particle velocities of different N with exactly the same tuning of the velocity gauge. It is for this purpose that the measurements were done with H^+ and He^+ ions with a large difference in $n = 2N - 1$. If X_1 and X_2 are the results of the two measurements of

$$X = \mu_P'/\mu_n \propto m/M$$

the true value of X will be

$$X = \frac{n_1 X_1 - n_2 X_2}{n_1 - n_2} \pm \frac{\sqrt{(n_1 \Delta X_1)^2 + (n_2 \Delta X_2)^2}}{n_1 - n_2} \tag{2}$$

where ΔX_1, ΔX_2 are errors entering statistically when switching from H^+ to He^+ (Section V).

iii) The last important source of systematic errors are spurious, neither a.f. amplitude nor velocity modulated r.f. background signals. Considering only the first important term of the Green function, the signal at the output of the first detector would be:

$$S_0 = |A_0(1 + \alpha_1 e^{-i\Phi})|^2.$$

If now the antenna or receiver input has a minute coupling to the deflection voltage oscillator it can pick up a second harmonic of frequency ω_0, amplitude B_0 and arbitrary phase φ, whereupon:

$$S = |B_0 e^{-i\varphi} + A_0(1 + \alpha_1 e^{-i\Phi})|^2.$$

Although the pickup signal is not a.f. modulated it contributes to a shift of the null phase by the component perpendicular to the true signal in the phase plane. With $A_0 \gg B_0$ one obtains:

$$\epsilon = -\frac{B_0}{A_0} \sin \varphi.$$

Careful shielding and decoupling can of course reduce B_0/A_0 to produce an insignificant error. A check for this condition was performed after each series of measurements
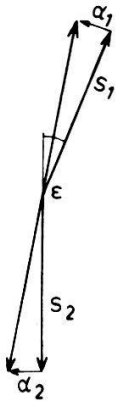
Figure 6
Effect of antisymmetric normal modes in complex phase plane.

(cf. Section III). It consisted of stopping the protons before the collimator and applying a 50% a.f. amplitude modulation to the r.f. deflector voltage without changing any existing coupling. This modulation was obtained from the a.f. generator of the phase sensitive detector on the gauge platform by an intensity modulated light beam. The absence of a shift of the detector null line was then observed at about five-fold increased sensitivity. A sufficiently small upper limit of ϵ is thereby obtained.

Further, but easier to account for, sources of systematic errors are:

i) Longitudinal acceleration of the ions by the r.f. modulation field. Due to the finite length of the deflector and its stray fields, ions passing through the collimator gain or lose momentum in the longitudinal direction. If the ions pass through perfectly symmetric fields and symmetrically in time with respect to the deflecting voltage zero, the effective velocity of the ions will still be the centroid of the velocity profile as measured by the magnetic spectrometer. However, large geometric asymmetries were present due to the fact that one deflecting plate was at ground potential. Effects of the above kind are of course proportional to the applied r.f. voltage, which for a given modulation index will be much smaller when the ion beam is focused on the collimator instead of on the centre of the gauge. Measurements showed that for even as high as 80% modulation, where the velocity profile splits already into two peaks, the centroid velocity remained unchanged, and up to 60% modulation no shift of the null condition within the desired accuracy was observed.
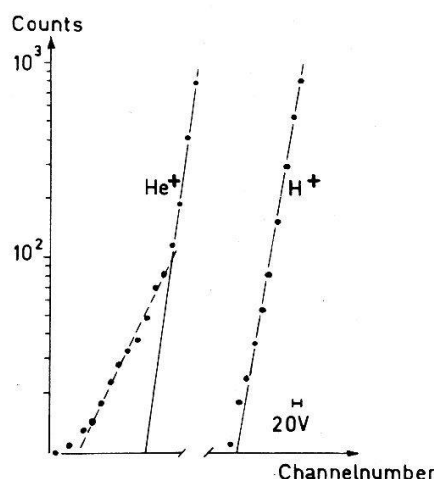

Figure 7
Low-energy tails of velocity profile in log scale. Maximum of distribution at 2000. For He⁺ the cutoff is indicated.

ii) Alteration of the velocity distribution by slit scattering between the velocity gauge and the magnetic spectrometer. Figure 7 shows a typical logarithmic plot of the low-energy side of the velocity profile for H^+ and He^+ ions. Whereas the asymmetric tail in the case of H^+ does not lower the centroid velocity significantly, the tail of the He^+ profile would indeed lower the centroid velocity by a few p.p.m. Since the main contribution to slit scattering occurs at the entrance slit system of the magnetic spectrometer, the tail of the He^+ profile was cut off in the manner indicated in Figure 7. Further justification of this procedure is given by the fact that the various He^+ results with different tails are internally consistent to better than 5 p.p.m. after application of the cutoff.

iii) Systematic errors in the magnetic field measurements. The quantity μ_p'/μ_n refers by convention to the Larmor precession frequency experienced by the protons in a spherical probe of pure water. As is well known the effective magnetic field, except for the molecular diamagnetic shift, is given by [13]

$$B = B_0 + (4\pi/3 - \alpha + q) \cdot M,$$

where B_0 is the field in pure water, $4\pi/3$ represents the Lorentz factor, α the demagnetizing factor given by the shape of the probe, q the shape-independent Dickinson factor and M the paramagnetic magnetization. The measuring probes were of spherical shape, $\alpha = 4\pi/3$, and q was determined separately with a high resolution n.m.r. spectrometer by comparing the 1/40 molar solution of $MnSO_4$ with pure H_2O in long transverse cylinders ($\alpha = 2\pi$). q was found to be $+0.50$, which is quite reasonable. For a spherical probe of 1/40 molar $MnSO_4$ solution the correction to B_0 is therefore only 0.16 p.p.m. and hence negligible. The finite susceptibility of the vacuum chamber material was likewise found to be negligible since the insertion of the chamber resulted in a field change of less than 1 p.p.m. As a further precaution the casings of the n.m.r. probes were made from the same wave guide material as the vacuum chamber. The spherical aberration of the 180° magnetic spectrometer is $\frac{1}{2}\vartheta^2$, where ϑ is the aperture angle. Collimation in the vertical and horizontal direction, particularly by the 90° aperture slit, ensures the shift due to spherical aberration to be less than 1 p.p.m. Likewise, the askew passage of the ions through the velocity gauge introduces an increase of the effective length of less than 1 p.p.m. Effects of bending under its own weight are entirely negligible for the drift tube as well as for the magnet slit system since, as for the latter, only distances between points of the neutral line are relevant. Dilatation of the magnet slit system due to the outside atmospheric pressure is also negligible. Since the n.m.r. probes measure the proton Larmor frequency corresponding to the total magnetic field B, while the orbital motion of the ions is determined by the component B_z only one has to measure or estimate the magnitude of components B_x and B_y. They can be obtained indirectly from the radial and azimuthal gradients of B which were always determined in connection with the determination of the Hartree correction. The biggest contribution arises from the almost uniform radial gradient of about 250 Hz/cm and amounts to less than 0.1 p.p.m. Finally, one has to consider curvature of the path of the ions in the velocity gauge due to magnetic fields, particularly the stray field of the magnetic spectrometer, and radial electric fields due to charges deposited on the walls of the magnetic spectrometer chamber. However, it turns out that neither of these effects can reach 1 p.p.m.

iv) As pointed out already by Altar and Garbuny [9], stationary oscillations of the velocity gauge cavity can also be excited by random current pulses through the gaps. In this case, however, the normal mode frequencies are excited and the interference minimum condition will be accordingly modified. In the present experiment it is the noise of the ion current which contributes to this type of oscillation. Since the output voltage of the gauge is fed to a narrow band r.f. amplifier, only that normal mode frequency ω_1 will contribute to which the r.f. modulation frequency ω_0 is tuned. If the tuning is exact no shift of the minimum condition will occur. If the r.f. modulated ion beam is of the form

$$I = I_0(1 + m \cos \omega_0 t)$$

a noise current $I^2(\omega)$ per unit frequency interval with a white spectrum will be present:

$$I^2(\omega) = I_0 \frac{e}{\pi} \cdot$$

It will extend up to a maximum frequency of the order

$$\omega_{max} = \frac{v_0}{d} \gg \omega_0,$$

where d is the gap distance, v_0 is the ion velocity and e the elementary charge. If ω_1 is the lowest normal frequency of the cavity, $\delta = (\omega_0 - \omega_1)/\omega_0$ the relative tuning deviation, b the relative bandwidth of the r.f. amplifier and Q the cavity Q value, calculation shows that the interference minimum is shifted by

$$\Delta v/v_0 = \frac{e\omega_0}{2\pi m^2 I_0}\left(\frac{1}{4Q^2} + \delta^2\right) \cdot F(b, \Delta, Q),$$

where the function F is of order 1 if b, Δ and $1/Q$ are all about equal and of order 10^{-4}. $\Delta v/v_0$ is therefore entirely negligible even for a large mistuning of the cavity to only 90% amplitude maximum.

V. Treatment of Data and Results

A total of fifteen complete determinations of the quantity $X = \mu_p'/\mu_n$ with protons and three with He^+ ions were carried out. The Hartree correction before and after the complete determination differed at most by 10 p.p.m. and if real was presumably caused by large temperature variations of the magnet during the measurement. For the evaluation of X for each series of one determination, the average value of the Hartree correction was used. For each series consisting of two null passages with positive drift tube voltage V_D occurring at the gauge step voltage V^+ and two with negative V_D at V^- it was ascertained that the quantity

$$\Delta = V_e^- - V_e^+ - 2V_D$$

was zero compatible with the accuracy of ± 6 V. Series for which Δ exceeded 16 V were rejected. The various series of a measurement were taken with different r.f. modulation index usually between 0.3 and 0.5. Every accepted series showed differences due to modulation of less than 10 V. For each passage the centroid voltage V_m was determined from the magnetic velocity profile. Finally, the series value of X was obtained from the two lengths L_0 and D appropriately corrected with the recorded temperature values and the two frequencies ω_m and ω_0 according to equation (1). The value of the mass ratio m/M for He^+ was calculated from the 1971 mass table [14], $m/M = 0.2516899$. The average serial results are presented in Table II.

The distribution of values of the individual passages fits a Gaussian $\exp(-\Delta X^2/2\sigma^2)$ about the average value $X = 2.792779$ and $\sigma = 0.000020$ extremely well except for values $\Delta X > \sigma$ where the observed numbers drop off symmetrically but much faster than the Gaussian. This however is not surprising since a number of errors are not of a purely statistical nature and, moreover, as mentioned above, values with large deviations of $\Delta = V_e^- - V_e^+ - 2V_D$ were discarded as possibly being affected by secondary electrons. From the data in Table II a weighted average was calculated in two different ways. First, only a weight factor g_3 equal to 1/4 of the number of zero passages was assigned to each series value and this yielded:

$H^+ : X = 2.792780$

$He^+ : X = 2.792776$

In the second averaging a product of three weight factors was used. In order to reduce the contribution of data with large differences in the initial and final values of the

Table II

Date	Ion	g_1	g_2	g_3	X
23/3/72	H$^+$	0.95	0.84	1.0	2.792767
		0.25	0.84	1.0	784
		0.95	0.84	1.0	772
5–8/5/72	H$^+$	0.61	0.97	4.0	780
		0.80	0.71	3.0	782
12–17/5/72	H$^+$	0.71	0.61	1.0	776
		0.65	0.61	1.0	772
		0.80	0.88	1.0	774
		0.70	0.88	1.0	777
		0.99	0.88	1.0	772
		0.55	0.98	1.0	770
		0.33	0.98	1.0	783
		0.80	0.98	1.0	779
		0.10	0.45	1.0	778
		0.65	0.45	1.0	781
		0.08	0.45	1.0	787
		0.03	0.45	1.0	797
		0.51	0.45	1.0	778
12–15/5/72	H$^+$	0.88	0.99	1.0	2.792783
		0.14	0.99	1.0	792
		0.07	0.99	1.0	796
		0.55	0.97	1.0	776
		1.00	0.97	1.0	768
		0.60	0.97	1.0	781
21/6/72	H$^+$	0.99	0.61	1.0	784
		0.60	0.61	1.0	793
		0.60	0.25	1.0	764
		1.00	0.25	1.0	777
2/7/72	He$^+$	0.95	0.71	3.0	774
		0.66	0.71	3.0	781
		0.25	0.10	1.0	766
		0.18	0.10	2.0	778

Hartree correction $\omega_m - \omega_m^0$, which was estimated to have a standard deviation of $\sigma_m/\omega_m = 4.7$ p.p.m., g_2 was given the corresponding Gaussian form

$$g_2 = \exp\left(-\Delta_\omega^2/2\sigma_m^2\right).$$

Finally g_1 was introduced to discriminate further against data affected with large values of $\Delta = V_e^- - V_e^+ - 2V_D$. Since the zero passage voltage V_e carries a statistical standard deviation $\sigma_e = \pm 6$ V:

$$g_3 = \exp\left(-\Delta^2/2\sigma_e^2\right).$$

With this averaging procedure one obtains:

H$^+$: $X = 2.792777$

He$^+$: $X = 2.792777.$

Therefore both procedures yield results well within the limits of the final error. Finally, the correction for excitation of higher modes according to equation (2) has to be made. Choosing the second more heavily weighted results, this correction is exactly zero with an uncertainty determined not by the actual errors of X_1 and X_2 but only certain statistical errors not recurring in the same manner in the H^+ and He^+ measurements. From the observed fluctuations we estimate for He^+, $n_1 = 25$; $\Delta X_1/X_1 = 2.4$ p.p.m.; for H^+, $n_2 = 11$; $\Delta X_2/X_2 = 1.3$ p.p.m.

Table III gives the list of errors and their magnitude (standard deviation).

Table III

1. step voltage values	0.4 p.p.m.
2. Frequency ω_m	0.8
3. Magnetic field configuration along actual particle orbit	4.7
4. Lengths L_0 and D with temperature correction	3.4
5. Asymmetries of gaps	1.0
6. Skewness of ion beam with respect to drift tube axis and stray fields	0.8
7. Non-spherical shape of n.m.r. probe and paramagnetic additive	2.0
8. Shift of V_e due to secondary electrons	2.3
9. Extrapolation of H^+ and He^+ to $1/n = 0$	2.0
10. Statistical error in V_e	0.2
Total standard deviation added quadratically	7.0

The values in Table III were obtained as follows:

1) The step voltages were measured to 1 V.
2) The frequency ν_m was manually kept constant to 20 Hz. The r.f. modulation oscillator for ω_0 had a frequency stability of 10^{-7}.
3) Deviation of actual orbit from nominal is estimated to be 0.5 mm, with an average radial gradient of 25 Hz/mm: 0.9 p.p.m. Uncertainty of azimuthal positioning of field measuring probe: 1.3 p.p.m. Over the large diameter of 1.2 cm of the probe the radial field gradient varied somewhat, shifting the effective centre of the probe and thereby causing an error of max. 2 p.p.m. Since these errors are at least partly correlated they were added linearly to 4.2 p.p.m. The n.m.r. signal had a width (f.w.h.m.) of 400 Hz. Its position could be read to 20 Hz. Together with asymmetries of the signal and scope non-linearities the error in reading the signal position is 2.0 p.p.m. Finally, the field configuration varied with temperature, introducing 1.0 p.p.m. error. The three effects are added quadratically to 4.7 p.p.m. in good agreement with the observed fluctuations of the Hartree correction.
4) Lengths L_0 and D were known to 2 and 3 μm respectively including uncertainties from temperatures.
5) Cf. Section III.
6) Gap hole diameter of 4 mm allows askew passage of ions, lengthening L_0 by 0.64 p.p.m. From the observed curvature of the ion beam further lengthening of 0.16 p.p.m. may be expected.
7) Cf. Section IV.
8) Cf. Section IV: Δ was determined to be 0 ± 6 V.
9) Cf. Section IV, equation (2).
10) Individual null passages could be determined to ± 6 V. A total of 180 passages was observed.

The final result using the triply weighted data is therefore:

$$\mu_{P'}/\mu_n = 2.792777 \pm 0.000020 \ (7 \ \text{p.p.m.})$$

in agreement with the provisional value [10].

In the meantime several new determinations of μ_P'/μ_n using low-energy ions have been reported and are listed in Table IV.

Table IV

1970 Fystrom [15]	Omegatron	2.792783 ± 0.000016 (6 p.p.m.)
1971 Mamyrin et al. [16]	Mag. Res. Mass. Spec.	2.7927745 ± 0.0000012 (0.43 p.p.m.)
1972 Luxon and Rich [17]	Mag. mirror well	2.792786 ± 0.000017 (6 p.p.m.)
1973 Petley and Morris [18]	Omegatron	2.7927748 ± 0.0000020 (0.72 p.p.m.)

All values, particularly those of Refs. [16] and [18], which are by an order of magnitude more accurate, are in perfect agreement with the present high-energy result, and are definitely higher than the previously accepted value [7] 2.792709 ± 0.000017 (6.2 p.p.m.)

Acknowledgments

APPENDIX

Theory of velocity gauge

Due to the well-defined symmetry centres of the field gaps, the velocity gauge can be represented as a one-dimensional, two-conductor infinite cutoff wavelength wave guide terminated capacitively and with variable capacitance $C(x)$, inductance $\mathscr{L}(x)$ and resistance $R(x)$ per unit length, satisfying the inhomogeneous equation for current and voltage

$$\frac{\partial V}{\partial x} + \mathscr{L}(x)\frac{\partial I}{\partial t} + R(x)I = 0; \quad \frac{\partial I}{\partial x} + C(x)\frac{\partial V}{\partial t} = j(x,t),$$

where $j(x)$ is the exciting current per unit length at x. $j(x,t) = 0$ everywhere except at end points x_1 and x_2 where a harmonically r.f. modulated ion current induces currents $J_1 e^{i\omega_0 t}$ and $J_2 e^{i\omega_0 t}$. Let ω_n be the normal frequencies of the system, u_n and v_n its orthonormal set of current and voltage eigenfunctions and $Q_n = \omega_n \overline{(\mathscr{L}(x)/R(x))}$. The Green function for V is:

$$G(x, x') = \sum_n \frac{\omega_n/\omega_0 v_n(x) u_n(x')}{\omega_0^2 - \omega_n^2 - i\omega_0 \omega_n/Q_n}$$

and

$$V(x) = \sum_n \frac{\omega_n/\omega_0}{\omega_0^2 - \omega_n^2 - i\omega_0\omega_n/Q_n}\,(u_n(x_1)\,J_1/C_1 + u_n(x_2)\,J_2/C_2), \qquad (3)$$

where C_1 and C_2 are the effective terminal capacitances. The radial stub antenna at x_0 will pick up a signal proportional to $V(x_0)$. The signal output of the first (square law) detector will be:

$$S \propto |V(x_0)|^2.$$

Referring to Figure 8, the exciting currents are obtained as follows: Let $n(t,v)$ be the number of ions with charge e emerging at time t with velocity v from the collimator at $x = 0$. Passing through point x of the first field gap at time t they will induce a current

$$J_1 = e \int_0^\infty \int_0^\infty n(t - x/v, v)\, f(x)\, dx\, dv,$$

where $f(x)$ is the value of the x component of the electrostatic field in x for unit potential across the gap. If x_1 is the coordinate of the geometric gap centre, $x = x_1 + \xi_1$, and
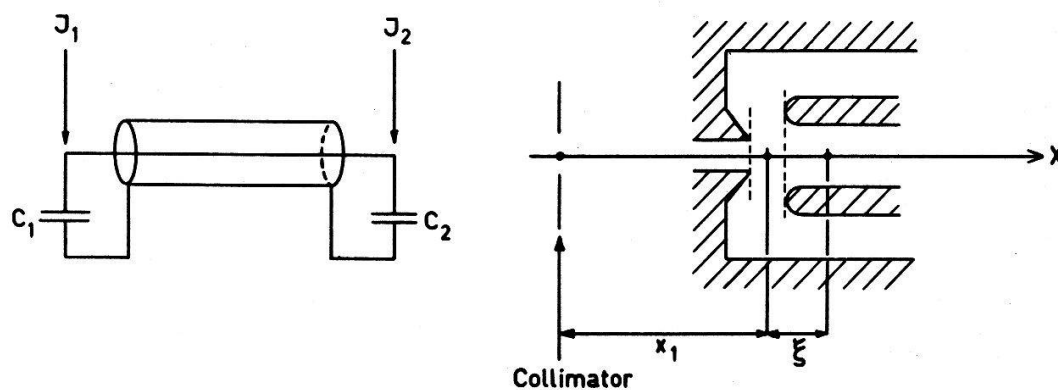

Figure 8
Schematic circuit of model and gap coordinates.

$f(\xi_1)$ differs from zero only for values $\xi_1/x_1 \ll 1$. Setting likewise $v = v' + \eta$ where v' is the velocity of the maximum of the distribution $n(v)$, this function will differ from zero only in a narrow region $\eta/v' \ll 1$. Since for the present experiment

$$\xi_1/x \approx 10^{-3}; \quad \eta/v' \approx 10^{-5},$$

quadratic and higher terms can be neglected, particularly since only odd powers contribute to the phase difference between J_1 and J_2. If $I_0(\omega_0)$ is the Fourier component with frequency ω_0 of the current emerging from the collimator, the components of $J(\omega_0)$ for $x = x_1$ and x_2 respectively are:

$$J(\omega_0) = I_0 \exp\left(-i\omega_0 \frac{(x + \bar{\xi})}{v' + \bar{\eta}}\right),$$

where

$$\bar{\xi} = \int_{-\infty}^\infty \xi f(\xi)\, d\xi$$

is the electrostatic centroid of the gap and

$$\bar{\eta} = \frac{1}{A} \int_{-\infty}^{\infty} \eta n(\eta) \, d\eta; \quad A = \int_{-\infty}^{\infty} n(\eta) \, d\eta$$

is the centroid velocity. Equation (3) can be written as:

$$V(x) = I_0 e^{-i\omega_0 \cdot x_1/v_0} \sum_n \frac{\mathrm{v}_n(x) \, \omega_n/\omega_0 \, u_n(x_1)/C_1}{\omega_0^2 - \omega_n^2 - i\omega_0 \omega_n/Q_n} (1 + \alpha_n e^{-i\Phi}). \tag{4}$$

$$\alpha_n = \gamma \frac{u_n(x_2)}{u_n(x_1)} \frac{C_1}{C_2}$$

is a real number with $\gamma \approx 1$ accounting for ions being lost in the drift tube and

$$\Phi = \frac{\omega_0}{v_0} (x_2 + \bar{\xi}_2 - x_1 - \bar{\xi}_1) = \frac{\omega_0 L_0}{v_0}. \tag{5}$$

$L_0 = x_2 + \bar{\xi}_2 - (x_1 + \bar{\xi}_1)$ is the effective electrical length and v_0 the centroid velocity: $v_0 = v' + \bar{\eta}$.

If I_0 is a.f. amplitude modulated,

$$I_0 = I_a(1 - m \cos \Omega t),$$

and only one normal mode is excited with frequencies ω_0, $\omega_0 \pm \Omega$,

$$S \propto m(1 + \alpha_1^2 + 2\alpha_1 \cos \Phi)$$

if small terms caused by the inherent phase modulation are neglected.
Minima are therefore obtained for $v_0 = v_0^0$ if

$$\Phi = \Phi_0 = (2N - 1) \pi = \frac{\omega_0 L_0}{v_0^0} \quad \text{where } N \text{ is an integer.}$$

In their neighbourhood S shows the parabolic dependence on $v_0 - v_0^0 = \eta_0$,

$$S \propto m(1 - \alpha_1)^2 + \alpha_1((2N - 1) \pi \eta_0/v_0^0)^2.$$

If v modulation is used,

$$v = v_0 + w \cos \Omega t = v_v(1 + m \cos \Omega t),$$

there are of course higher order side bands present. Since m is extremely small of order 10^{-5} they can be neglected and the output signal is:

$$S \propto 2\alpha_1 \frac{\omega_0 L_0}{v_0} m \sin \Phi$$

with nulls for

$$\Phi = \Phi_0 = N\pi = \frac{\omega_0 L_0}{v_0^0}.$$

In the neighbourhood of a minimum zero:

$$v_0 - v_0^0 = \eta_0.$$

S will vary linearly

$$S \propto 2\alpha_1 m((2N - 1)\pi)^2 \eta_0/v_0^0.$$

The advantages of velocity modulation are the very small modulation index, the absence of other modulation types and higher sensitivity since instead of a minimum signal a true null signal has to be observed.

REFERENCES

[1] J. B. Marion and H. Winkler, Phys. Rev. *156*, 1062 (1967).
[2] H. Sommer, H. A. Thomas and J. A. Hipple, Phys. Rev. *82*, 697 (1951).
[3] J. H. Sanders and K. C. Turberfield, Proc. Roy. Soc. (London) *A272*, 79 (1963).
[4] B. W. Petley and K. Morris, Proc. Third Int. Conf. on Atomic Masses, Winnipeg, 1968.
[5] B. A. Mamyrin and A. A. Frantsuzov, Sov. Phys. J.E.T.P. *21*, 274 (1965).
[6] H. S. Boyne and P. A. Franken, Phys. Rev. *123*, 242 (1961).
[7] W. H. Parker, D. N. Langenberg, A. Denenstein and B. N. Taylor, Phys. Rev. *177*, 639 (1969).
[8] J. D. Seagrave, J. E. Brolley and J. G. Beery, Rev. Sci. Inst. *35*, 1290 (1964).
[9] W. Altar and M. Garbuny, Phys. Rev. *76*, 496 (1949).
[10] H. Gubler, W. Reichart, M. Roush, H. Staub and F. Zamboni, Proc. of the Int. Conf. on Precision Measurements and Fundamental Constants, Gaithersburg, 1970.
[11] L. A. West, Thesis, Univ. of Maryland, Dept. of Physics, 1969.
[12] H. Winkler and W. Zych, Helv. Phys. Acta *34*, 449 (1961).
[13] W. C. Dickinson, Phys. Rev. *81*, 717 (1951).
[14] A. H. Wapstra and N. B. Gove, Nuc. Data Tables *9*, 265 (1971).
[15] D. O. Fystrom, Phys. Rev. Lett. *25*, 1469 (1970).
[16] B. A. Mamyrin, N. N. Arujev and S. A. Alekseenko, Proc. Fourth Conf. on Atomic Masses and Fundamental Constants, Teddington, 1972.
[17] J. L. Luxon and A. Rich, Phys. Rev. Lett. *29*, 665 (1972).
[18] B. W. Petley and K. Morris, J. Phys. A. (G.B.) **1973**.